FA 12.8 CIRRUS AND CONTRAIL MICROPHYSICAL PROPERTIES DERIVED FROM SATELLITE DATA DURING SUCCESS

D. F. Young, P. Minnis
Atmospheric Sciences Division
NASA Langley Research Center, Hampton, Virginia

W. L. Smith, Jr., R. Palikonda, and L. Nguyen
Analytical Services and Materials, Inc., Hampton, Virginia

1. INTRODUCTION

Contrails are a special class of cirrus clouds that form in an environment rich in potential cloud condensation nuclei compared to the conditions generating most typical natural cirrus clouds. The contrails may persist and develop into clouds that are indistinguishable from their non-anthropogenic counterparts. When formed within extant cirrus, contrails may alter the microphysical properties of the host cirrus leading to changes in the cloud lifetime or optical properties. The presence of contrails, therefore, may have a significant effect on the radiation budget. One goal of the NASA Subsonic Assessment (SASS) program is to estimate the impact of contrails on the Earth's radiation budget and their role in climate change. The Subsonic Aircraft Cirrus and Contrails Special Study (SUCCESS) field experiment was conducted under the auspices of SASS and the First International Satellite Cloud Climatology Project (ISCCP) Regional Experiment (FIRE) during Spring 1996 over the U.S. to better understand the composition, radiative properties, and life cycles of cirrus and high-altitude aircraft exhaust and its associated contrails. This paper examines the life cycles of several contrail-cirrus cloud systems and explores differences in the optical properties of cirrus and contrails as determined from satellite observations taken during and after SUCCESS.

2. DATA AND ANALYSIS METHODS

Areal coverage, effective ice crystal diameter D_e, heights z, and optical depth τ for both cirrus and contrail-cirrus are derived from multi-spectral, 1-km Advanced Very High Resolution Radiometer (AVHRR) and 4-km Geostationary Operational Environmental Satellite (GOES) data. Analyses of the AVHRR data are used to determine the contrail properties during the early stages of their development. Several distinct contrail systems are tracked with the GOES as they develop and dissipate. Apparently natural, nearby cirrus are analyzed for comparison. The NOAA-12/14 AVHRR data used here comprise the visible (VIS; 0.65 μm), solar-infrared (SI; 3.7 μm), infrared (IR; 10.8 μm), and split window (WS; 12.0 μm). The GOES imagers have similar channels except that the SI central wavelength is 3.9 μm. Data were taken from both GOES-8 at 75°W and GOES-9 at 135°W. Temperature was converted to altitude using soundings from the nearest National Weather Service station.

Both constant and variable box sizes were used to analyze a particular feature and to isolate the clouds arising from the subject contrail systems. The box selection also includes portions of the background to compute the clear-sky VIS clear-sky reflectance and IR, SI, and WS clear-sky temperatures T_{CS}. During daytime, the VIS-IR-SI technique (VIST) was used to determine the values for each parameter, while the SI-IR-WS (SIRS method) was applied at all hours (Minnis et al., 1995). The cloudy pixels were identified over ocean as those having temperatures $T < T_{CS}(IR) - 1.5K$. Over land, the temperature threshold depression varies up to 6K depending on the variability of the backround temperature. For contrail systems, the parameters were computed only for the pixels corresponding to the contrail cloudiness. Screening other cloudy pixels is mostly subjective, however, some objective criteria were applied to eliminate non-contrail clouds. Clouds with temperatures $T_C > 273K$ were assumed to be low clouds and clouds with $\tau > 1$ were assumed to be pre-existing cirrus. Cloudy pixels with indeterminate particle size results were assumed to belong to the contrail because those results usually occur for optically thin clouds or because the particles were smaller than the smallest ice crystal model. The areal contrail coverage is the number of contrail pixels multiplied by the mean area of a pixel at the given viewing angle.

3. RESULTS

During the SUCCESS experiment conducted over the U.S., two distint contrail systems were observed off the coasts. One was a series of figure eights from an unknown source over the Gulf of Mexico during 11 April (Fig. 1). The eights were originally 30 km wide and extended ~70 km from north to south. During a 11 May 1996 SUCCESS flight, the NASA DC-8 produced a 100-km-long oval over the Pacific Ocean as it sampled contrails produced by commercial airliners and its own

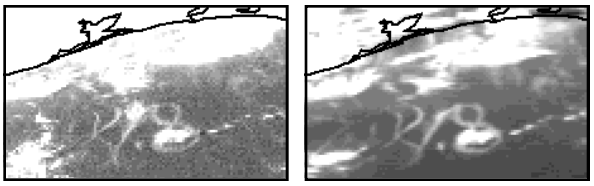

a) VIS b) IR

Fig. 1. GOES-8 4-km imagery at 2015 UTC, 11 April 1996 showing figure-eight contrails over the Gulf of Mexico.

*Corresponding author address: Patrick Minnis, MS 420, NASA Langley Research Center, Hampton, VA 23681-0001; email <p.minnis@larc.nasa.gov>.

a) VIS b) IR c) T(IR) - T(WS)

Fig. 2. GOES-9 4-km imagery at 2315 UTC, 12 May 1996 off the coast of California. (a) Oval shows DC-8 flight track from 2250-2315 UTC.

exhaust (Fig. 2). These two sets of contrails are ideal for tracking because they are extensive and easily distinguishable from natural clouds. Linear contrails produced by commercial aircraft over the east coast of the U.S. on 26 September 1996 comprise the third case. These are seen in their early stages over the mouth of the Chesapeake Bay in the AVHRR imagery in Fig. 3.

To demonstrate the analysis procedure, Fig. 4 shows the two-dimensional histograms of the data for the linear contrails (Fig. 3). Lines showing some of the model results for water droplets and ice crystals are also given. These models correspond to the mean cloud temperatures and particle sizes determined with the VIST by forcing the results to be either liquid or ice particles. As seen in Fig. 4a, solutions exist for both ice and liquid particles for these contrail clouds when only the IR and SI data are considered. Because T_c(liquid) = 272K, the unconstrained VIST would have selected the liquid phase for this case. However, a comparison of the model results with the IR-WS histograms shows that the liquid cloud cannot explain the data, while the ice cloud with D_e = 21 μm, τ = 0.3, and T_c(ice) = 216K provides an excellent fit to the data. This temperature corresponds to an altitude of 11 km on the 1200-UTC sounding taken at nearby Wallops Island, Virginia. This height, ~36,000 ft, is much more reasonable for commercial air traffic than the 11,500 ft corresponding to 272K. These same contrails were also observed to be at high altitudes from the surface. Analyses of the apparently natural cirrus clouds at the north end of the bay and over land south of the bay both yielded D_e = 55 μm, slightly lower atitudes, and $\tau \sim 0.6$.

The VIST ice and liquid models for the IR, VIS, and SI have considerable overlap, especially in the small ice-particle, low optical depth ranges (D_e < 30 μm, τ < 2). As the results in Fig. 4b clearly indicate, the contrails are composed of small ice crystals that are less than half the size of the nearby cirrus clouds. To prevent phase misidentification in the remaining analyses, the VIST contrail analyses use only the ice models to determine cloud particle sizes.

Analysis of NOAA-14 AVHRR data taken at 1915 UTC, 11 April 1996 over the Gulf of Mexico, early in

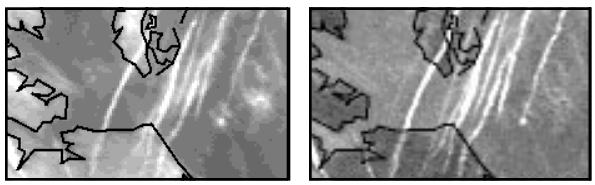

a) IR b) T(IR) - T(WS)

Fig. 3. NOAA-12 1-km imagery at 1214 UTC, 26 September 1996 showing lower Chesapeake Bay.

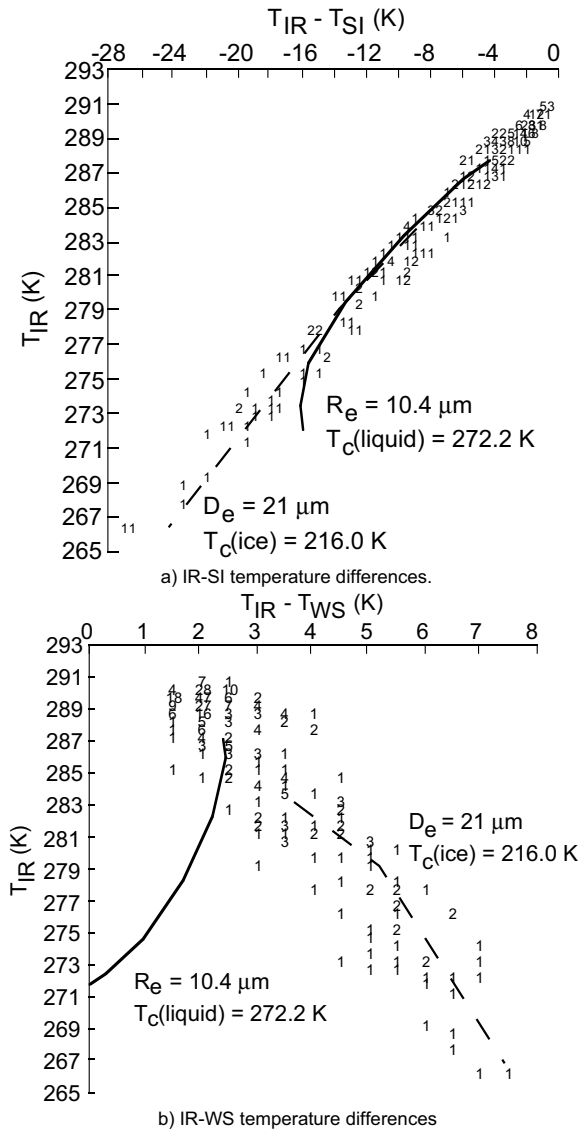

Fig. 4. Brightness temperature differences for contrail scene over mouth of Chesapeake Bay in Fig. 3. Model fits are based on mean of pixel-by-pixel VIST analysis.

the development of the figure-eight contrail, yielded z = 7.5 km, τ = 0.2, and D_e = 23 μm. The altitude (~26,000 ft) is based on the 1200-UTC, 11 April sounding taken at Lake Charles, Louisiana. The troposphere above 7 km was extremely moist indicating that the derived height is reasonable for contrail formation. The leading (easternmost) edge of the eastern eight had D_e = 30 μm while the crystal sizes were smaller than 20 μm on the western side where z varied from 6 - 9 km. The transformation and dissipation of the figure-eight contrails can be seen in Fig. 5. At 2045 UTC, the arms of the eights were 2-4 pixels or ~12 km wide. The eights gradually diffused, filled, and became indistinguishable from other cirrus by 2245 UTC. They advected ~750 km before disminishing to a small area south of the Florida panhandle by 0145 UTC, 12 April. During most of that time, the contrail clouds were too wide or dispersed to

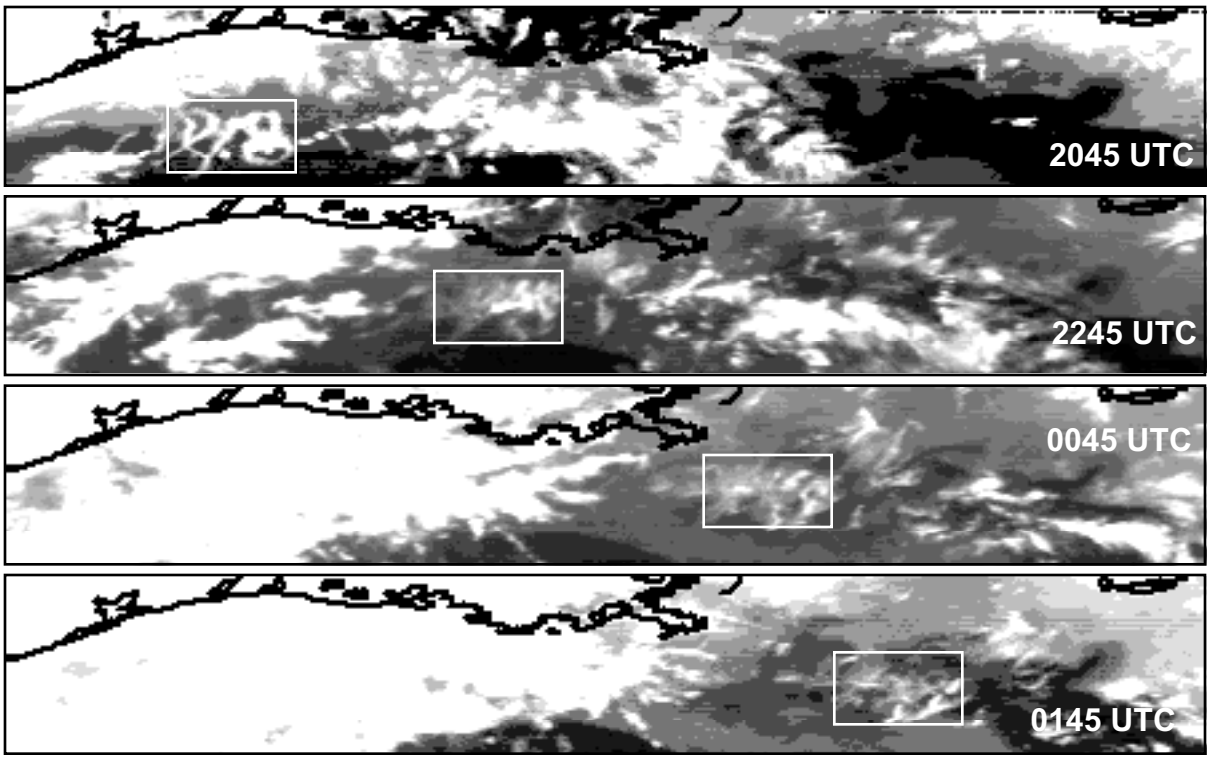

Fig. 5. GOES-8 infrared imagery over the Gulf of Mexico showing development and dissipation of the figure-eight contrails, 11-12 April 1996.

be recognizable as contrails from the satellite or the surface. Figure 6 shows the analysis results using the two techniques applied to the GOES data within the analysis boxes. The VIST cloud temperature increased slightly after 3 hours suggesting that the contrail dropped in altitude as it spread. Optical depth remained relatively constant. The SIRS analysis yields different values for the cloud parameters. T_c decreases until 2115 UTC before increasing again. Although the initial values are nearly the same, the optical depths are smaller and D_e is larger, on average, than the VIST results. The SIRS analysis is less reliable during the day than at night so the retrievals after 0000 UTC are more accurate. When lower clouds are absent, the VIST results are more accurate than the SIRS data. Thus, the parameter variations given by the VIST are a better representation prior to 2300 UTC. The results for τ and D_e after 2300 UTC are probably accurate to ± 50%. The areal coverage increases steadily until it reaches ~24,000 km^2 at 0000 UTC. The mean contrail cloud optical depths decreased after 0000 UTC as the cloud dissipated.

As seen in Fig. 2, the scene containing the DC-8 contrail is very complex. It formed over a background of low stratocumulus and advected over a clear portion of the ocean along the coast before passing over land at 0045 UTC, 13 May (Fig. 7). The contrail also fills and spreads as it moves with the wind. At 0400 UTC, over the foothills of the Sierra Nevada, the racetrack shape disappears, replaced by a somewhat amorphous shape. When the system reaches the mountains (0445 UTC), the cloud seems to thicken before dissipating over Nevada at 0545 UTC. The analysis results in Fig. 8 show the cloud starting near 230 K and apparently dropping in altitude to warmer temperatures. The

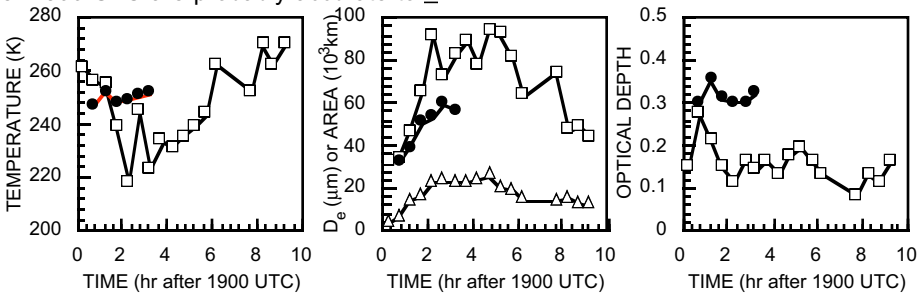

Fig. 6. Cloud parameters from figure-eight contrails over Gulf of Mexico for 11-12 April 1996. Closed symbols from VIST analysis. Open symbols from SIRS. Triangles refer to area.

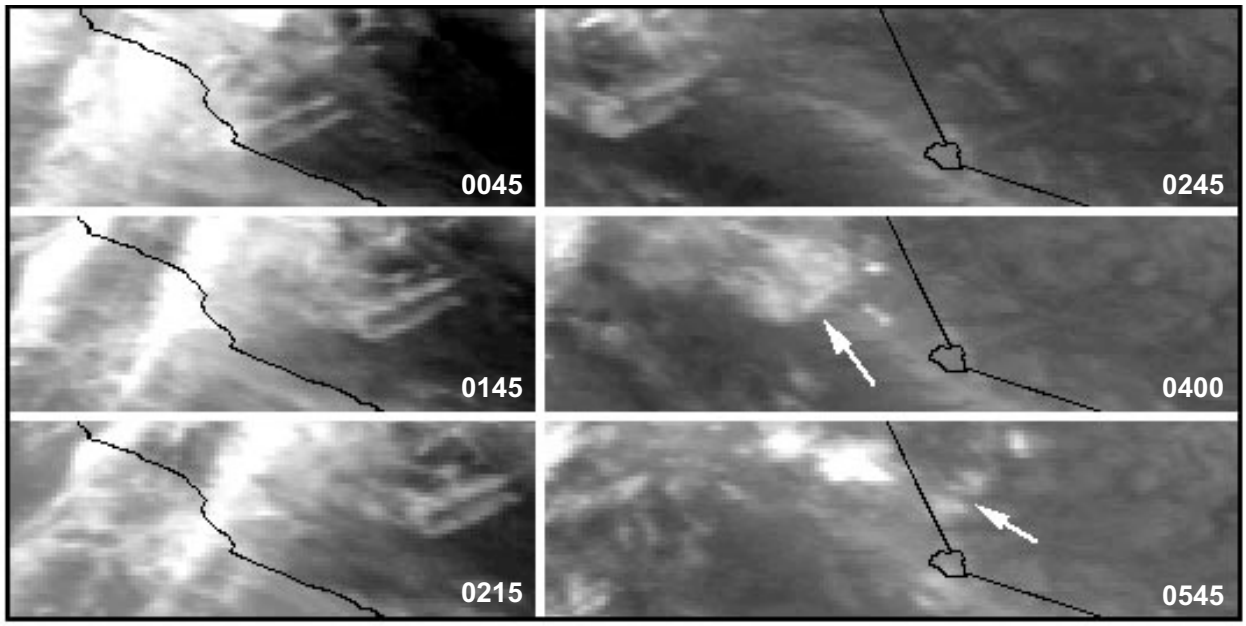

Fig. 7. GOES-9 IR imagery showing transformation and dissipation of the DC-8 racetrack contrail, 13 May 1996, over Northern California to Nevada border.

particle size initially is ~30 μm, increasing to ~ 40 μm for several hours and to larger values over the mountains. Data between 2330 and 0115 UTC are not included because the background was too variable. Analysis of the contrail sections only over the clear ocean at 0045 UTC yield D_e = 46 μm, although some of the pixels had particle sizes between 20 and 30 μm. The optical depths in Fig. 8, which average ~ 0.5, far exceed those seen for the figure-eight contrails. Areal coverage by this contrail-cirrus system reaches a peak of ~ 5000 km^2 at 0230 UTC. The DC-8 flew at an altitude near 10 km which corresponds to ~229K on the nearest sounding. Thus, it appears that T_C for the contrail was overestimated by more than 10K for much of the cloud's lifetime. The magnitude of this potential error is not surprising given the changing background.

The linear contrails in Fig. 3 were tracked and analyzed over the Atlantic Ocean with a constant-area box using GOES-8 data (Fig. 9). The derived cloud temperature is erratic initially, then remained relatively steady near 245K for the rest of the period. The temperatures correspond to z = 8.5 km almost 3 km lower than the initial AVHRR retrieval. Like the previous two cases, the mean particle sizes increase from very small values to those more typical of natural cirrus, but decrease again after 1530 UTC. The contrails in Fig. 3 were observed from the surface around 1230 UTC and occurred with scattered, thin natural-looking cirrus. Therefore, it is possible that the higher temperature at 1245 UTC may be due to analysis errors arising from the uncertain background temperature. The optical depths are significant, averaging around 0.3 for the study period. The contrails appear to have developed from ~33% coverage in the box at 1215 UTC to 80% 6 hours later. Examination of the surrounding areas in the GOES-8 imagery yielded little cirrus coverage. These same parts of the air mass lacked the original contrails seen at 1230 UTC in the AVHRR imagery suggesting that the contrails were responsible for much of the observed cloudiness in the box which was generally clear before 1200 UTC.

4. DISCUSSION

Accurate determination of the cirrus microphysical properties is difficult for clouds with such small optical depths. The sensitivity of the retrievals to variations in background reflectance and temperatures is greatest when the clouds are thin (τ < 0.5). However, the effective particle sizes in Figs. 6, 8, and 9 change as expected for contrails. Initially, very small particles form because of the abundance of nuclei. As the cloud diffuses into cleaner air, crystal growth ensues. The different behavior seen in Fig. 9 may be due to errors in the clear-sky values after 1500 UTC. A closer examination of the data is required to determine if the retrievals are accurate. The DC-8 took microphysical measurements during the initial formation of that contrail, so it will be possible to estimate the retrieval errors for the first few data points.

Errors in cloud height are also difficult to ascertain. The actual altitude of figure-eight contrail is unknown, although a plane flying such a papttern is likely to stay out of typical commercial flight altitudes. Given the sounding and this consideration, the 7.5 km height is reasonable. Some of the apparent underestimation of the racetrack cloud height may be due to changes in the cloud or uncertainties in the background radiances. Because the contrail area and particle sizes grow rapidly, the mean height may decrease because of precipitation into lower layers. Visual observations from the DC-8 note that the contrail was precipitating shortly

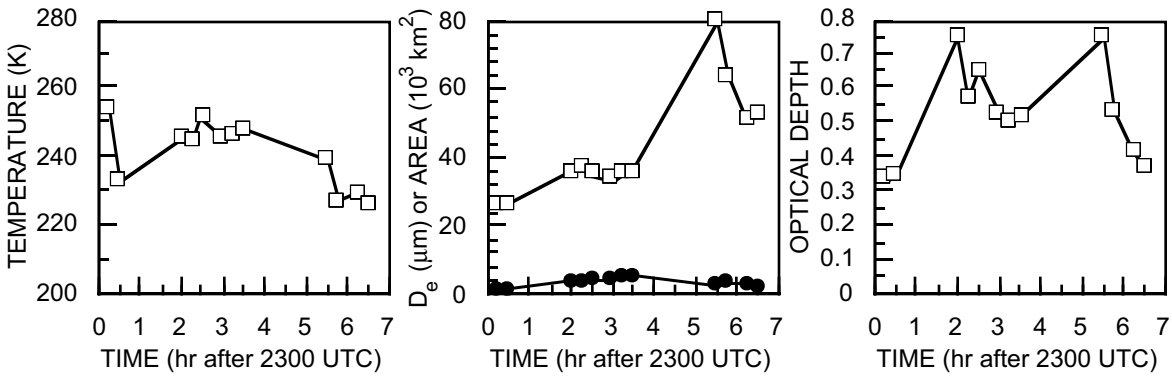

Fig. 8. Cloud parameters computed for racetrack contrail from GOES-9 data 12-13 May 1996. Solid symbols refer to contrail area. Temperature refers to contrail temperature.

after its formation. Additionally, the value of T_c for very thin clouds is closer to the base of the cloud than the top. Estimation of the cloud top temperature from the optical depth and T_c yield $z \sim 10.5$ km early in the cloud's development.

The cloud growth rates seen in Figs. 6, 8 and 9 are remarkable. Peak coverage occurs approximately 3 hours after the contrail is detectable from the satellite. The contrail clouds dissipate slowly both in horizontal and vertical extent. The contrail lifetimes were not totally observed in these results. Significant areal coverage remained in all three cases after 5 to 9 hours. Additional re-growth or continued dissipation is possible. Assumptions about contrails remaining in the air routes are not supported by these results. Contrail cloudiness can advect considerable distances from their source, substantially increasing the area affected by manmade clouds.

5. CONCLUDING REMARKS

It is clear from these results that contrail areal coverage is much greater than that derived from analyses relying on the narrow linear features typically associated with contrails in satellite imagery. Such analyses provide only a minimum estimate of contrail cloud cover. The results found here are not necessarily typical of all contrails. Given the difficulty in analyzing these relatively distinct cases, it may be concluded that objective tracking or automated retrieval of advecting contrail properties will require substantial additional research. Until more automated procedures become available, it will be possible to acquire a more representative statistical base of contrail characteristics by performing analyses similar to the present one using a much larger satellite dataset. Such statistics are crucial elements for understanding the impact of contrails on climate. This study is just an initial glimpse of the potential changes in cloudiness induced by modern air travel.

6. REFERENCES

Minnis, P., D. P. Kratz, J. A. Coakley, Jr., M. D. King, R. Arduini, D. P. Garber, P. W. Heck, S. Mayor, W. L. Smith, Jr., and D. F. Young, 1995: Cloud optical property retrieval (Subsystem 4.3). "Clouds and the Earth's Radiant Energy System (CERES) Algorithm Theoretical Basis Document, Volume III: Cloud Analyses and Radiance Inversions (Subsystem 4)", NASA Reference Paper RP-1376 Vol. 3, 135-176.

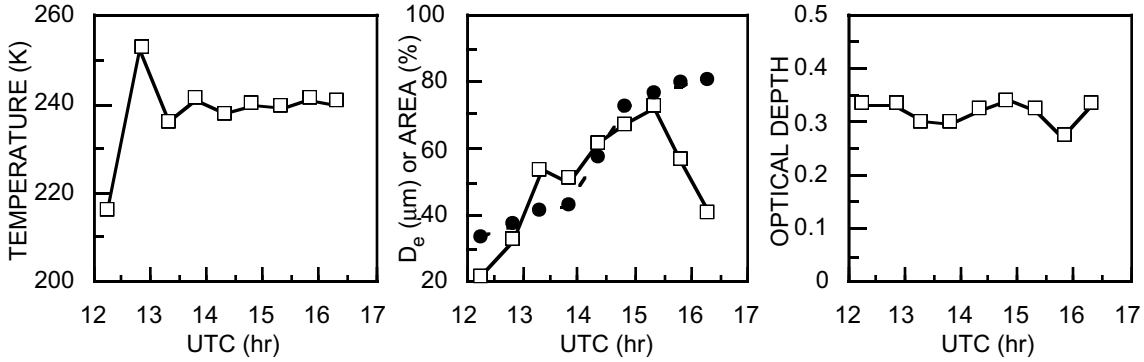

Fig. 9. Cloud parameters computed from AVHRR and GOES-8 data with VIST for a moving 20x30 pixel box containing contrails during 26 September, 1996. Temperature refers to cloud temperature. Solid symbols are for area.